≪Research Paper≫ Applied Science and Convergence Technology Vol.23 No.2, March 2014, pp.97~102
http://dx.doi.org/10.5757/ASCT.2014.23.2.97

Design and Fabrication of a Vacuum Chamber for a Commercial Atomic Force Microscope

Sang-Joon Park[a], Yeon-Uk Jeong[b], Soyeun Park[c], and Yong Joong Lee[a]*

[a]*School of Mechanical Engineering, Kyungpook National University, Daegu 702-701*
[b]*School of Material Science and Engineering, Kyungpook National University, Daegu 702-701*
[c]*College of Pharmacy, Keimyung University, Daegu 704-701*

(Received February 7, 2014, Revised March 21, 2014, Accepted March 26, 2014)

A vacuum chamber for a commercial atomic force microscope (AFM) is designed and fabricated. Only minimal modifications were made to an existing microscope in an effort to work in a vacuum environment, while most of the available AFM functionalities were kept intact. The optical alignment needed for proper AFM operations including a SLD (superluminescent diode) and a photodiode can be made externally without breaking the vacuum. A vacuum level of 5×10^{-3} torr was achieved with a mechanical pump. An enhancement of the quality factor was observed along with a shift in the resonance frequency of a non-contact-mode cantilever in a vacuum. Topographical data of a calibration sample were also obtained in air and in a low vacuum using the non-contact mode and the results were compared.

Keywords : Vacuum chamber, Atomic force microscope, Quality (Q) factor

I. Introduction

Since the invention of the first atomic force microscope (AFM) by Binnig, Quate, and Gerber in 1986, many experiments have been carried out with atomic force microscopes [1]. Unlike the scanning tunneling microscope (STM) invented earlier, AFMs are capable of obtaining various surface properties of electrically insulating materials. Despite being initially applied to physics and material science experiments, AFMs are now well-adopted instruments in biology and related areas [2-4]. AFMs are often compared to optical microscopes and scanning electron microscopes (SEM). However, an AFM has superior lateral and vertical resolutions compared to an optical microscope and can operate in an ambient condition, unlike a SEM. For these and other reasons, AFMs have been one of the most frequently utilized instruments in nano-science and engineering. Recently, there have been attempts to probe the electrical, optical, and mechanical properties of organic devices [5-9]. Due to a common requirement for an inert or oxygen-free environment for the proper operation of many organic devices, there is now an increased level of demand for specialized environmental AFMs [10]. However, except for a few expensive and very specialized ultrahigh-vacuum and environmental AFMs, most commercial AFMs are designed to operate under am-

---

* [E-mail] yjlee76@knu.ac.kr

bient conditions.

In this study, we designed and constructed a vacuum chamber for a commercial AFM (XE-70, Park Systems). This is a much better cost-effective strategy for adding an environmental control faculty to a commercial AFM system as compared to designing an entirely new AFM system operable in a vacuum. A calibration sample was scanned both in air and in a vacuum and the results are compared.

II. Experimental Procedures

First, the XE-70 device was analyzed thoroughly in terms of its structure and functionalities. Then, various parts of the XE-70 were categorized as essential or non-essential. Essential parts were to be installed inside the chamber and non-essential parts were to be removed from the AFM and installed outside of the chamber or not used at all. Given that our set goal was not in designing a completely new vacuum-compatible AFM, most of the essentials parts were kept without any modifications. A Z-scanner head which contains a SLD (superluminescent diode), a four-quadrant photodiode and beam steering mirrors was kept intact. Also the stepper motor-driven vertical stage for the Z-scanner head was kept in order to retain the automatic-sample-approach functionality. In order to reduce the overall height of the vacuum chamber, the original optical microscope was removed due to its long length and its objective lens with a limited working distance of 33.5 mm. However, the optical alignment, i.e., moving a SLD spot to the tip of a cantilever, can be quite difficult without the help of an optical microscope. Thus, a machine-vision microscope with a color CCD with a working distance of more than 300 mm replaced the original optical microscope. Although the working distance was greatly increased, the numerical aperture (NA) of the vision system was decreased such that the overall magnification with the new microscope is only 1/5 of the original system. We found that optical alignment was still possible, as shown in Fig. 1. The focused SLD spot could be clearly located at the tip of the cantilever. Further fine tuning could be done by reading the sum signal from the four-quadrant photodiode available from the AFM control software. We also explored the application of a simple two-lens Galilean telescope and successfully observed a SLD spot on a cantilever. Either microscope system can be installed on a three-axis translation stage such that precise positioning control would be possible with respect to the cantilever mount inside the vacuum chamber.

The optical alignment of the XE-70 is done by rotating a set of four precision screws placed on the Z-scanner head, two on the top and two on the side of the Z-scanner. Because the Z-scanner head was installed inside the vacuum chamber, an external control mechanism for these screws was needed. As shown in Fig. 2, ball-end hex keys were welded at the ends of the vacuum feedthrough rods first. Also, the caps for the precision screws were designed and installed. These caps have socket head screws that

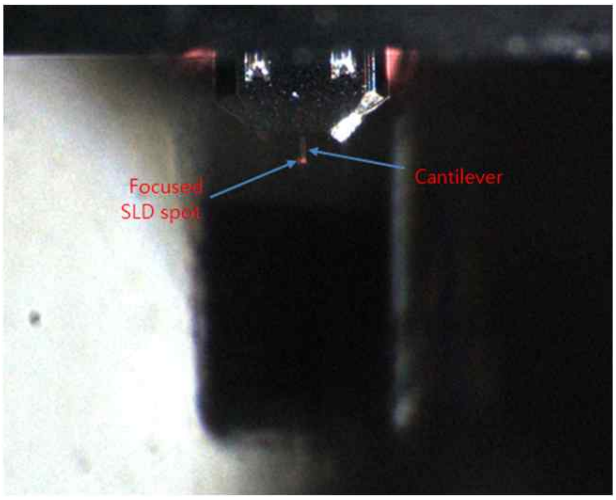

Figure 1. SLD spot aligned at the tip of an intermittent-contact-mode AFM cantilever as observed with a microscope installed with a CCD.

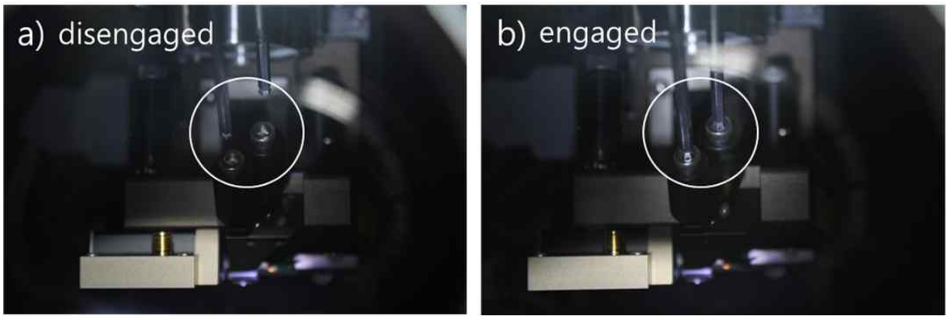

Figure 2. Two feedthrough rods with hex ball ends as seen through the front chamber viewport. Feedthrough rods a) disengaged and b) engaged from the beam−steering mirror−adjustment screws.

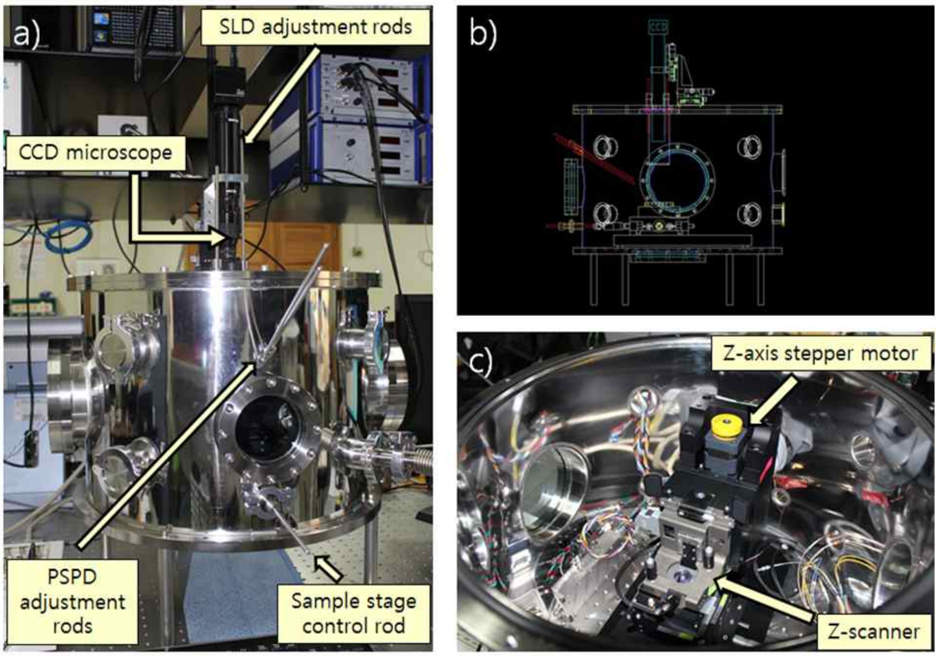

Figure 3. a) Front view of the vacuum chamber. Various feedthrough rods and a CCD camera system on the top of the chamber can be seen. b) Right−side view of the CAD drawing of the vacuum chamber. The front, side, and bottom viewports can be seen. Although an XE−70 AFM drawing is not shown, the sample stage and scanner can be seen in relation to the optical microscope setup. c) An internal view of the chamber showing the installed XE−70 AFM with various electrical wires.

can be mated with the hex keys welded to the feedthrough rods inside the vacuum chamber. Once the hex keys and socket head screws are mated, precision alignment screws can be turned from the outside of the vacuum chamber by rotating the feedthrough rods. After the alignment was carried out, some lengths of the feedthrough rods can be pulled outside of the vacuum chamber to decouple the feedthrough rods from the sensitive optical alignment screws completely. The ball−end hex keys allow this control scheme to work well even if a feedthrough rod and a mating screw are not perfectly aligned. A misalignment of up to 20° was found to be tolerable for proper operation. The same external control scheme was applied to a sample coarse−positioning stage controlled by a set of two micrometers.

Fig. 3 shows the constructed vacuum chamber and the AFM installed inside the chamber. For convenient optical access, four viewports (front, left, right, and bottom) with diameters larger than 90 mm were installed. The bottom viewport could be especially useful for combined optical and AFM studies if an open−center sample scanner is installed in the future. Also, KF−40 flanges were regularly placed around the chamber wall for future expandability. Using these extra ports, additional sensors or the use of an introduced gas would be possible for customized experiments.

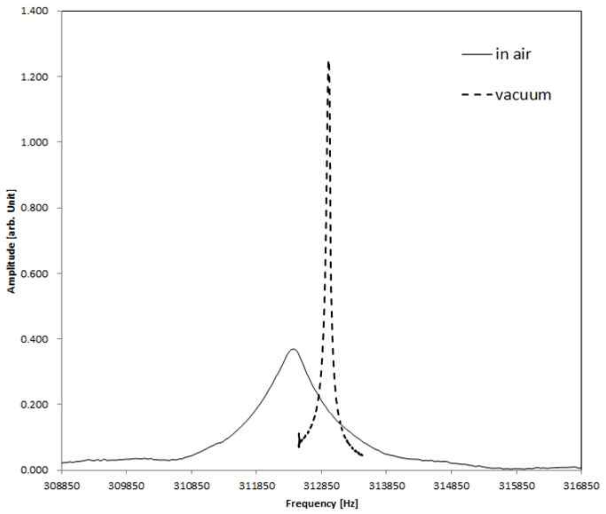

Figure 4. Piezo−driven resonance curve of a typical non−contact−mode cantilever in air (solid line) and in a vacuum (broken line) at 8×10^{-3} torr. A clear enhancement of the quality factor (Q) and a shift in the natural resonance frequency can be observed.

III. Results and Discussion

A vacuum level of 5×10^{-3} torr could be achieved with a mechanical pump. The quality factor (Q) of a AFM cantilever is strongly dependent on the pressure. Generally, the lower the pressure, the higher the values of the quality factors which are observed. However, for a pressure level below the molecular flow regime ($<1\times10^{-4}$ torr), the quality factor improvement becomes nearly stagnant [11]. Therefore, one must carry out non−contact or inter−mittent−contact AFM experiments after the pressure

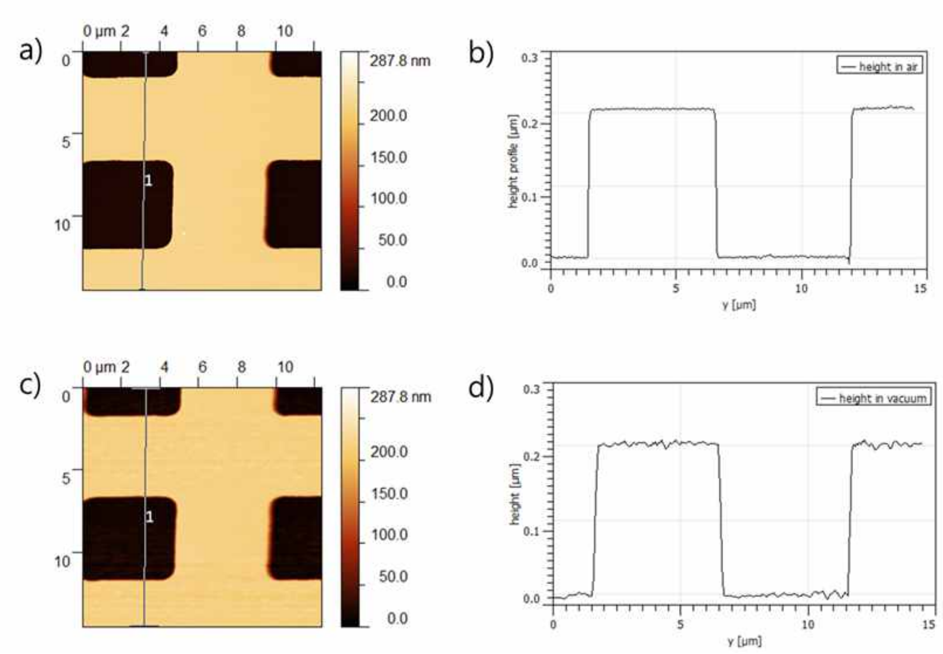

Figure 5. a) Topography of a calibration sample measured in air. b) Cross−sectional profile along the line shown in a). c) Topography of a calibration sample measured at 1× 10−2 torr. d) Cross−sectional profile along the line shown in c).

has been stabilized if the experiments are done in a viscous flow regime ($>1\times10^{-4}$) torr). Otherwise, non-existent interactions could appear in the AFM data as actual features despite the fact that they are caused by the cantilever's changing intrinsic properties. Fig. 4 shows two piezo-driven resonance curves for the same cantilever in air and a pressure of 8×10^{-3} torr. The quality factors in air (solid line) and in a 8×10^{-3} vacuum (broken line) were calculated to be 397 and 4325, respectively. A clear quality factor enhancement was observed along with a shift in the resonance frequency typical for a non-contact AFM cantilever [11].

In order to achieve a vacuum level below 1×10^{-3} torr, a high-vacuum pump such as a turbomolecular or a diffusion pump is needed. However, for the verification of the operability of the AFM system in a vacuum, we probed a standard AFM calibration sample in a low vacuum. Fig. 5 shows the non-contact-mode topographical data obtained from the calibration sample (10 μm pitch, 200 nm depth) at a vacuum level of 1×10^{-2} torr. The topographic images a) and c) were captured in air and in a 1×10^{-2} torr vacuum, respectively. The graphs of b) and d) show cross-sectional profiles along the lines shown in the corresponding topographic images. Both sets roughly show the correct pitch and depth values. However, the background noise characterized by the arithmetic mean roughness (R_a) shows a large difference. The calculated values for the arithmetic mean roughness in air and in a vacuum were found to be 0.61 nm and 14.1 nm, respectively. We attribute the greater than 20-fold increase in the roughness to the mechanical and acoustic vibrations caused by the mechanical pump connected to the vacuum chamber. The in-air experiments were carried out with the pump turned off while the in-vacuum experiments require the continuous use of the mechanical pump.

An installation of a much less vibrant turbomolecular pump along with a vibration filtering mechanism for the mechanical pump is underway in order to lower the background vibrational noise level. Fig. 6 shows the proposed vacuum line connections from the vacuum pumps to the chamber containing the AFM. The use of long flexible bellows and the introduction of a heavy mechanical damper unit will help the overall noise level reach a value close to the in-air value measured with the vacuum pumps turned off. However, there is a trade-off when using long bellows. The overall pump-down time will increase with an increase in the length of the bellows used for connections. An optimal balance between the pump-down time and the background vibration noise level must be found. We also expect that the constructed vacuum chamber can be used as an environmental chamber to provide a gaseous environment in addition to a vacuum environment upon the installation of proper gas introduction valves for studying various samples.

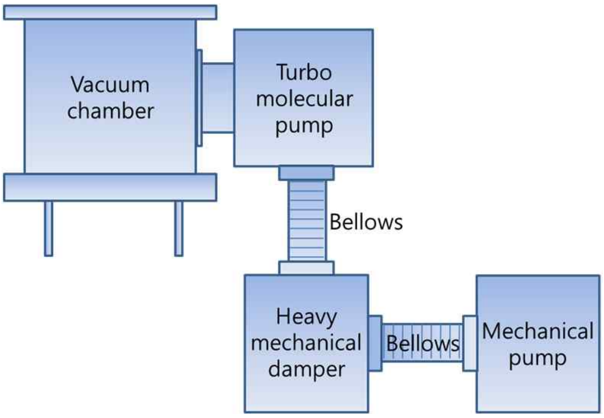

Figure 6. Proposed vacuum line connections to minimize the mechanical vibration from the vacuum pumps. Relatively large vibrations from a mechanical pump are initially filtered by a heavy damper. The transfer of vibration from the vacuum pumps is further minimized by flexible bellows where appropriate.

IV. Conclusion

In conclusion, we designed and constructed a vacuum chamber for a commercial XE-70 AFM from Park Systems. Only minimal modifications to the AFM were made while keeping most of the essential AFM features intact. The vacuum chamber includes four viewports for external viewing and extra blank ports in the event of future expansions. External manipulation of precision alignment screws is possible without breaking the vacuum with custom-made feedthrough rods with hex keys. The XE-70 AFM was installed in a vacuum chamber and the chamber was evacuated to 5×10^{-3} torr with a mechanical pump. An enhancement in the quality factor and a shift in the resonant frequency of a non-contact-mode AFM cantilever were successfully observed. Topographic data for a calibration sample were obtained in air and in a vacuum and the results were compared.

Acknowledgements

This research was supported by the Kyungpook National University Research Fund of 2010.

References

[1] G. Binning, C. F. Quate, and Ch. Gerber, Phys. Rev. Lett. **56,** 930 (1986).

[2] G. Binnig, H. Rohrer, Ch. Gerber, and E. Weibel, Phys. Rev. Lett. **49,** 57 (1982).

[3] S. Kasas, N. H. Thomson, B. L. Smith, P. K. Hansma, J. Miklossy, and H. G. Hansma, Int. J. Imaging Syst. Technol. **8,** 151 (1997).

[4] K. C. Chang, Y. W. Chiang, C. H. Yang, and J. W. Liou, Tzu Chi Medical Journal **24,** 162 (2012).

[5] P. A. Cox, D. A. Waldow, T. J. Dupper, S. Jesse, and D. S. Ginger, ACS Nano **7,** 10405 (2013).

[6] G. Shao, G. E. Rayermann, E. M. Smith, and D. S. Ginger, J. Phys. Chem. B **117,** 4654 (2013).

[7] N. Balke, D. Bonnell, D. S. Ginger, and M. Kemerink, MRS Bulletin **37,** 633 (2012).

[8] R. Giridharagopal, G. E. Rayermann, G. Shao, D. T. Moore, O. G. Reid, and D. S. Ginger, Nano Letters **12,** 893 (2012).

[9] C. Groves, O. G. Reid, and D. S. Ginger, Accounts of Chemical Research **43,** 612 (2010).

[10] J. Lievonen, K. Ranttila, and M. Ahlskog, Rev. Sci. Instrum. **78,** 043703 (2007).

[11] J. Lubbe, M. Temmen, H. Schnieder, and M. Reichling, Meas. Sci. Technol. **22,** 055501 (2011).